



Microstructure and mechanical properties of austenitic steel EK-164 after warm rolling

S. A. Akkuzin^{†,1}, I. Yu. Litovchenko¹, A. V. Kim², E. N. Moskvichev¹, V. M. Chernov³

[†]s.akkuzin@ispms.ru

¹Institute of Strength Physics and Materials Science, SB RAS, Tomsk, 634055, Russia

²National Research Tomsk State University, Tomsk, 634050, Russia

³A. A. Bochvar High-Technology Research Institute of Inorganic Materials, Moscow, 123098, Russia

The influence of warm plastic deformation by rolling on the microstructure and mechanical properties of an austenitic reactor steel is investigated. It is shown that a high total strain degree ($\epsilon = 2$) contributes to the elongation and flattening of austenite grains in the rolling direction. The average grain size decreases from 19.3 μm (in the solution treated state) down to about 0.5 μm . Near the elongated grain boundaries many fine grains with a diameter of less than 0.5 μm are detected. These grains are formed by dynamic recrystallization. The structural states formed in the steel provide high strength properties: the yield strength increases up to the values of 800 MPa at 20°C and 530 MPa at 650°C, which are 4 and 5.6 times higher than in the solution treated state, respectively.

Keywords: austenitic steel, warm rolling, microstructure, electron microscopy, electron backscatter diffraction, grain refinement, strength.

1. Introduction

The austenitic chromium-nickel steel EK-164 is currently used as a cladding material for fast-neutron reactor fuel elements [1,2]. Due to special operating conditions of fuel assemblies (elevated temperature gradient, stress gradient along the entire length of the assembly, corrosive effects of coolant and high damaging radiation doses) higher mechanical properties are required for the reactor-grade steels. Various thermal and thermo-mechanical treatments (TMTs) represent a method to modify the microstructure of austenitic steels and increase their mechanical properties [3–6]. Earlier [7,8], we performed thermomechanical treatments of EK-164 steel including low temperature, cold and warm plastic deformation by rolling on of EK-164 steel. Following the treatments, the total strain degree was found to be $\epsilon \approx 1$ (where ϵ is the true strain). It was shown that plastic deformation at the temperatures of 20°C and lower gave rise to the formation of a microtwin structure in steel EK-164 [8]. The presence of a high density of deformation twins and the formation of shear bands make it possible to increase the yield strength of steel up to 1050 MPa and the tensile strength up to 1230 MPa [7,8]. However, this strengthening also considerably reduces the elongation to failure down to about 4%. During plastic deformation at higher temperature (600°C), twinning is suppressed, grain fragmentation is initiated and a banded substructure is formed. In this case, the elongation to failure of steel increases and is not less than 6% [8]. In addition, according to [9], the twin microstructure has increased thermal stability, and a complete recrystallization of the microstructure is possible only near temperatures of 1000°C. A microstructure without deformation twins can have higher values of the elongation

to failure. Recrystallization in this structure occurs at lower temperatures.

It is known that plastic deformation at elevated temperatures (600–1100°C) can increase the strength of austenitic steels while maintaining ductility at a high level [10–15]. In addition, at elevated deformation temperatures (above 600°C) there is a possibility of dynamic recrystallization (DRX) processes in austenitic steels [15–17]. It is shown that the dynamic recrystallization process is possible only at high strain degree ($\epsilon \geq 2$). The deformation rate and temperature are also important parameters. The formation of a duplex structure with DRX grains and highly deformed grains can provide increased strength and ductility in austenitic steels.

In the present work, the influence of thermomechanical treatments with warm plastic deformation by rolling ($\epsilon \approx 2$) on the features of the microstructure and mechanical properties of the austenitic steel EK-164 is investigated.

2. Materials and experimental methods

The material used was Russian grade austenitic reactor steel EK-164 (Fe-17.92Ni-15.93Cr-2.4Mo-1.74Mn-0.68Si-0.4Ti-0.28Nb-0.12V-0.07C, mass.%). Prior to deformation, the samples were solution treated (ST) at 1100°C for 1 hour followed by water quenching. Heating was carried out in a tubular electric furnace of the T-40/600 type. The rolling mill was maintained at room temperature. The initial sample size was 54×10×10 mm³. TMTs consisted of plastic deformation by rolling in 6 passes (at a total strain degree of $\epsilon \approx 2$) with preheating to $T = 600$ (TMT-1) or 900°C (TMT-2). The holding time of the samples in the furnace at these temperatures was 10 minutes. The time between removal of the samples from the furnace and the beginning of plastic

deformation was about 3–5 seconds. After removal from the mill, the samples were quenched directly in water. The final thickness of the samples after thermomechanical treatment was 1.37 mm.

The microstructural characterization was performed using an Apreo 2 S high-resolution scanning electron microscope (SEM) equipped with a Field Emission Gun, an Octane Elect Super energy-dispersive spectral (EDS) analysis detector and a Velocity Super electron backscatter diffraction (EBSD) system. The SEM samples were prepared by mechanical polishing followed by ion milling as a final polishing step. Ion polishing was performed using a Technoorg Linda SEMPRep 2 system. The EBSD images were taken from the longitudinal (perpendicular to transverse direction) and parallel to the rolling plane (perpendicular to normal direction) sections. Further, these sections are designated as TD and ND, respectively. The EBSD data for TMT-1 and TMT-2 were obtained with a step size of 50 nm for the areas of 100 μm^2 .

Transmission electron microscopy (TEM) investigations were conducted using a Philips CM-12 electron microscope at an accelerating voltage of 120 kV. Thin foils were prepared from the sections perpendicular to TD by electropolishing in an electrolyte containing 450 ml of orthophosphoric acid and 50 g of chromic anhydride.

Mechanical tests were carried out at room temperature (20°C) and high temperature close to the maximum operating temperature (650°C) by the method of static tensile deformation at a strain rate of $2 \times 10^{-3} \text{ s}^{-1}$ on a NIKIMT 1246R-2/2300 high-temperature vacuum testing machine. Dogbone shaped samples with a gage length of 13 mm and a gage section of $2 \times 1 \text{ mm}^2$ were used. The samples were cut from the sections parallel to the rolling plane and perpendicular to ND. High temperature tensile tests were carried out in a vacuum of $2.5 - 3.5 \times 10^{-5} \text{ Pa}$.

3. Results and discussion

The results of the study on the microstructure of steel EK-164 in the ST state by SEM EBSD methods were presented in detail elsewhere [18]. It was shown that the initial microstructure was presented by the austenite with the average grain size of about 19.3 μm . Within the grains, there are numerous special type boundaries corresponding to the annealing twins. The fraction of these boundaries is 68%. It is noted that the fraction of high-angle boundaries is about 97%, and that of the low-angle boundaries is 3%. The average grain size is 7.7 μm including twin boundaries. The SEM-EDS and TEM-EDS analysis showed that inside the grains there were complexly alloyed particles of the MC type, where M is Nb, Ti, V or Mo [18,19]. The content of these elements in carbides varies regardless of their sizes.

The use of TMT with plastic deformation by rolling at $T = 600^\circ\text{C}$ (TMT-1) results in a fragmentation of the austenite grains and an increase in the density of high- and low-angle boundaries (Fig. 1). The fragmentation of the structure in the section perpendicular to the ND demonstrates a certain heterogeneity. There are areas with fine grains only and areas consisting of coarse (up to 23.4 μm) grains (Fig. 1a). The average grain size is about 0.48 μm . The fraction of high-

angle (above 15°) boundaries is equal to 29.4%. The fraction of low-angle (from 2 to 15°) boundaries is 70.6%. The fraction of twin boundaries decreases to less than 1% compared to the initial state. This is due to the high deformation degree ($\epsilon = 2$) at elevated temperatures. Figures 1b and 1c show the microstructure and density of the high- and low-angle boundaries in more detail. Note the presence of fine (less than 0.5 μm) almost equiaxed grains both in small clusters and individual grains which are located at the boundaries of coarse grains (Fig. 1c).

The feature of the microstructure in the section perpendicular to TD is the reduction in the longitudinal grain size and grain elongation in the rolling direction (Fig. 1d–f). The average grain size is about 0.4 μm . Figure 1d shows a banded structure consisting of elongated grains with different thicknesses. This is due to the heterogeneous deformation and to different orientations of the initial grains with respect to RD and ND. The fraction of high-angle boundaries is 33.3%, and that of low-angle boundaries is 66.7%. The magnified image (Fig. 1f) of the microstructure highlighted in Fig. 1e shows that along the coarse (from 0.5 to several μm thick) elongated grains there are many equiaxed grains with the diameters smaller than 0.5 μm . Within the coarse elongated grains, a large number of low-angle misorientation boundaries are present.

In these two microstructure sections, the relative frequency of fine grains exceeds 70%.

Thermomechanical treatment with plastic deformation by rolling at $T = 900^\circ\text{C}$ (TMT-2) results in similar changes in the microstructure of the steel as in the case of TMT-1. The difference in microstructure is related to the sizes of the structural elements. After TMT-2, in the section perpendicular to the ND, the microstructure of the steel consists of fragmented grains of a few micrometers in size and grains up to 0.5 μm in size (Fig. 2a). The fractions of these grains are 20% and 80%, respectively. The average grain size is 0.53 μm . At the same time, individual coarse grains with sizes up to 24.5 μm were detected. Within the coarse grains, multiple low-angle boundaries (Fig. 2b, c) and individual fine grains (up to 1 μm) are detected. The fractions of high-angle and low-angle misorientation boundaries are 30 and 70%, respectively.

In the section perpendicular to the TD a banded structure is observed (Fig. 2d–f). The average grain size is 0.57 μm . The austenitic grains have a specific shape of long elongated plates. They can be up to 70 μm in length. The structure contains mainly grains up to 1 μm wide, but individual grains with a width of 10–15 μm can also be found. It should be noted that the fine grains are located along the elongated coarse grains (Fig. 2f). The fraction of high-angle boundaries is 47% and that of low-angle boundaries is 53%. The fraction of fine grains is 62%.

The features of the microstructure after TMT-1 and TMT-2 in the sections perpendicular to TD were investigated by transmission electron microscopy (Fig. 3). A fragmented banded microstructure consisting of elongated subgrains (plates) with predominantly low-angle misorientation boundaries forms as a result of TMT-2. The average width of these plates is $\approx 330 \text{ nm}$. Nanosized carbide particles can be found inside the plates. Plastic deformation at 600°C (TMT-1) results in the formation of narrower elongated plates. Their

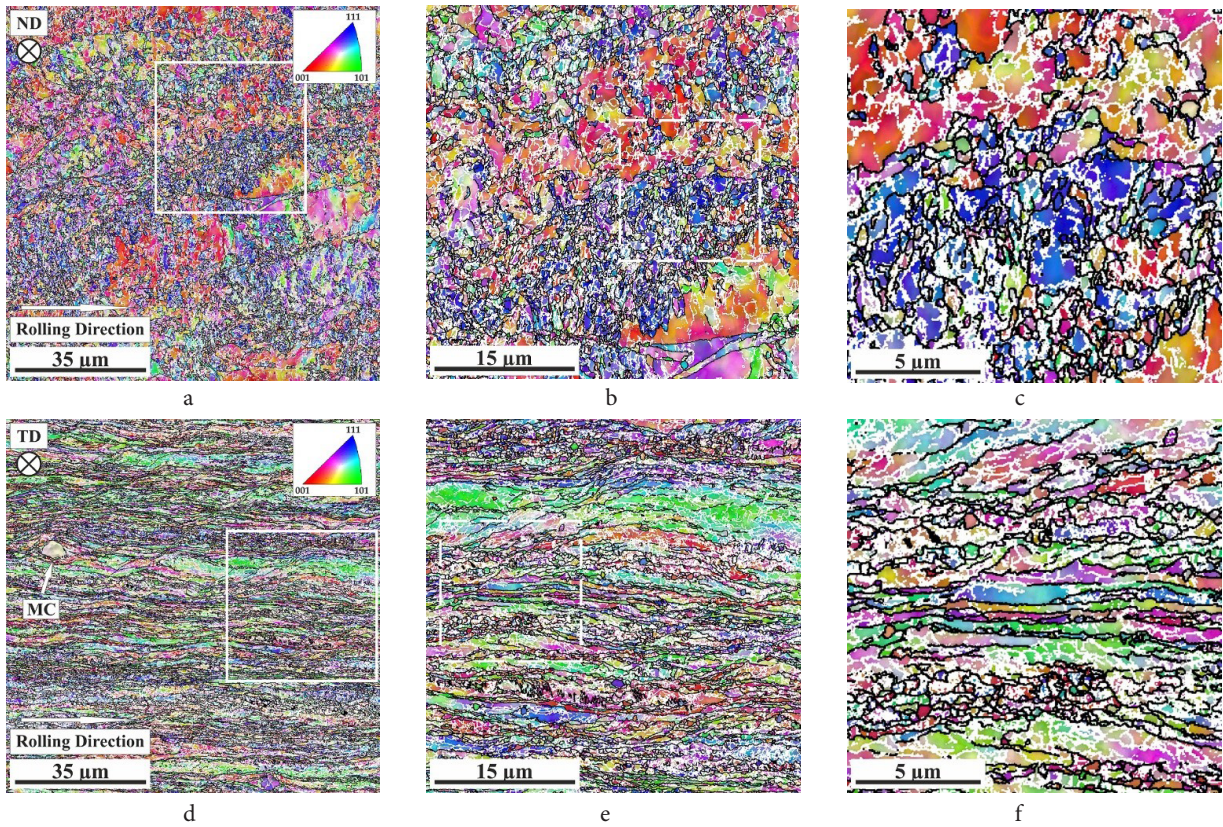


Fig. 1. (Color online) Electron backscattered diffraction (EBSD) images of the steel microstructure after TMT-1. Orientation maps (a–f), where black and white lines denote high-angle and low-angle boundaries, respectively. First magnified images (b, e) are parts of the images (a, d), marked up with a white solid frame. Second magnified images (c, f) are parts of the images (b, e), marked up with a white dashed frame. The arrow in (d) indicates coarse carbide MC.

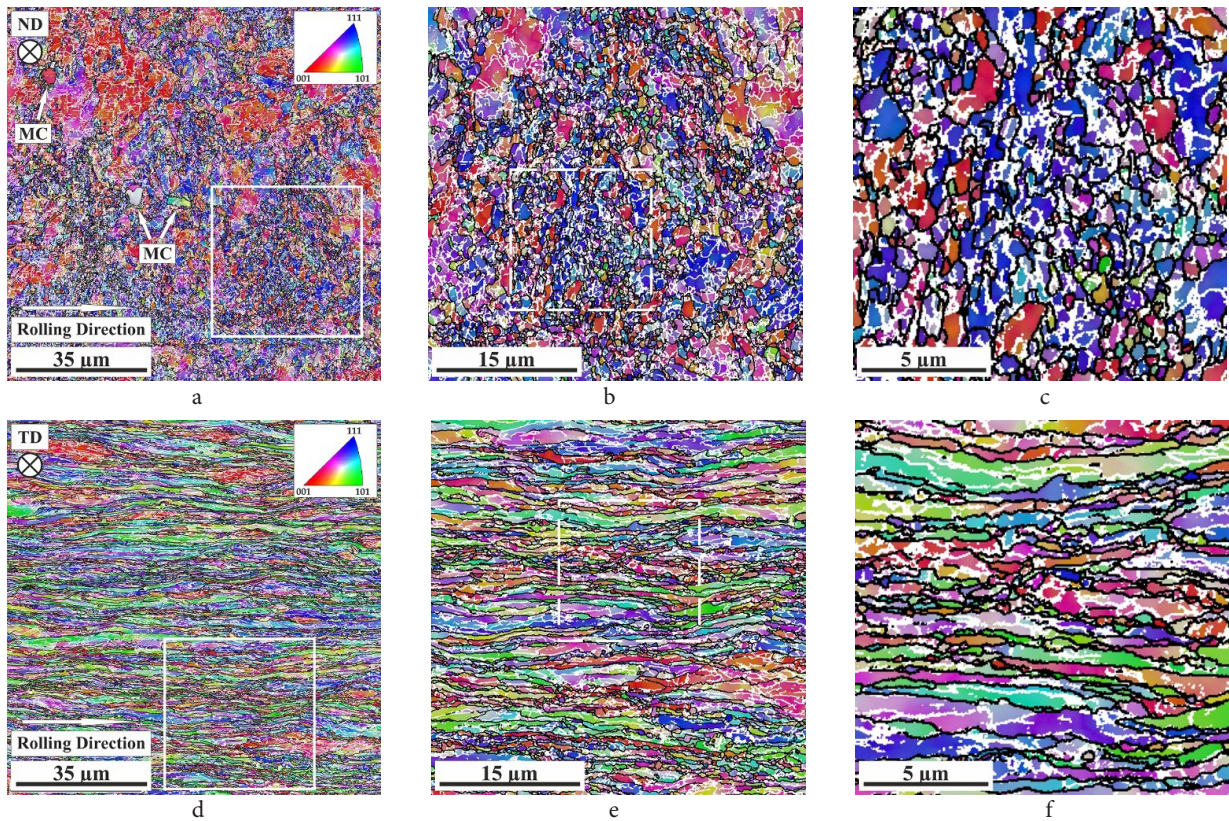


Fig. 2. (Color online) EBSD images of the steel microstructure after TMT-2. Orientation maps (a–f), where black and white lines denote high-angle and low-angle boundaries, respectively. First magnified images (b, e) are parts of the images (a, d), marked up with a white solid frame. Second magnified images (c, f) are parts of the images (b, e), marked up with a white dashed frame. The arrows in (a) indicate coarse carbides MC.

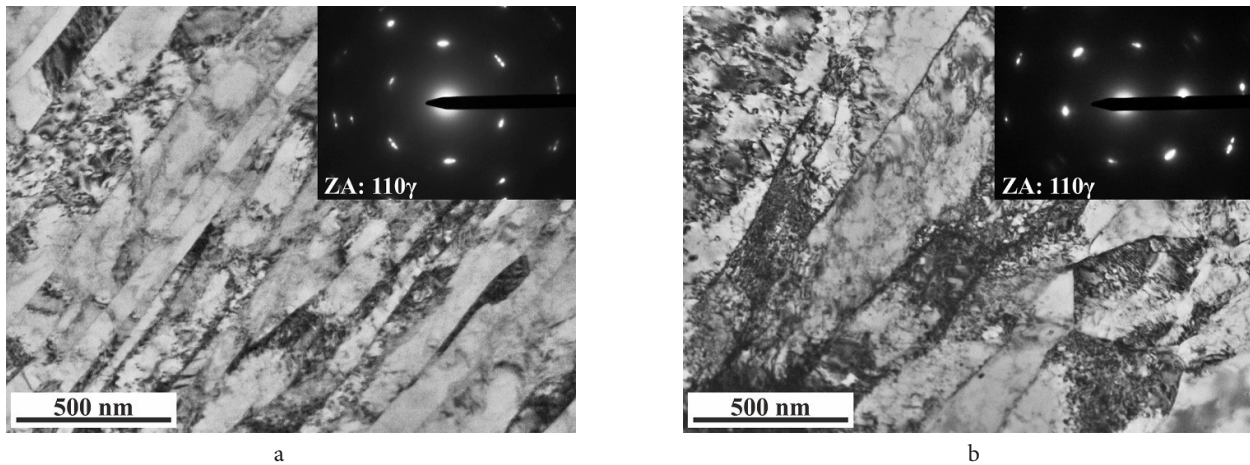


Fig. 3. Transmission electron microscopy images of steel microstructure after TMT-1 (a) and TMT-2 (b). Bright-field images with a selected area electron diffraction pattern, zone axis $[110]\gamma$ is indicated.

average width is 150 nm. The analysis of the diffraction patterns shows the presence of zone axes close to $\langle 110 \rangle \gamma$, as well as high-angle and low-angle misorientation boundaries.

The mechanical properties of the steel in the ST and after TMTs are shown in Table 1. In ST state, the typical mechanical properties of the austenitic steels are observed at 20°C. At elevated (650°C) tensile temperatures, the mechanical properties of EK-164 steel have a feature — in addition to lower values of yield and tensile strength there are lower values of elongation to failure (Table 1). This material behavior is associated with the development of dynamic strain aging, which manifests itself in the form of serrated plastic flow over almost the entire length of the tensile curves for this state. The mechanism of the dynamic strain aging is presented and discussed in detail in [18]. TMT-1 leads to an increase in strength — the yield strength of steel increases by a factor of 4 (at 20°C) and 5.6 (at 650°C) compared to the ST state. The elongation to failure is reduced down to 7% both at 20°C and at 650°C. The use of TMT-2 at higher deformation temperatures leads to a lower yield strength of the steel — the yield strength increases up to 741.9 MPa (at 20°C) and up to 500.8 MPa (at 650°C). The elongation to failure is 8% (at 20°C) and 5% (at 650°C). The minor differences in the properties after TMT-1 and TMT-2 are due to the grain sizes and to the number of high- and low-angle misorientation boundaries. It should also be mentioned that during heating of the steel specimens to the temperature of $T = 900^\circ\text{C}$ (after the first and the following passes) the processes of partial softening of structure took place, because this temperature is higher than the temperatures of the beginning of static recrystallization

and recovery processes. These processes lead to a decrease of the fraction of low-angle boundaries and, accordingly, an increase of the fraction of high-angle boundaries.

Thus, as a result of TMTs, fragmented microstructures with grains flattened and elongated along the rolling direction were formed. Earlier, this microstructure was designated as pancake grain structure [10,18,20]. Many fine grains smaller than 1 μm were detected at the boundaries of elongated grains (plates). Their formation is often associated with dynamic recrystallization processes [17]. One of the mechanisms of formation of these grains is bulging of boundaries. The grain boundaries first extend along the rolling direction and then bend under plastic deformation with the increasing strain degree, and finally bulge, indicating strain-induced grain boundary migration [16,17,21,22]. This deformed microstructure provides improved strength properties while maintaining elongation to failure at an acceptable level (Table 1). The achieved strength properties after TMT-1 are slightly higher (yield strength by approximately 40 MPa) than in [18], where a multistage high-temperature TMT with a temperature reduction was applied with $e \approx 2$. It should be noted that in the present work the average grain size was 3.6 times smaller than in [18] and grain structure was more homogeneous.

4. Conclusions

The influence of thermomechanical treatments with warm plastic deformation by rolling on the microstructure and mechanical properties of the austenitic steel EK-164 has been investigated. It has been shown that after warm rolling with a high strain degree of $e \approx 2$ a fragmented banded microstructure with a well-developed substructure and fine grains is formed. The average grain size is 0.5 μm . The fine grains located at the boundaries of elongated grains are formed in during dynamic recrystallization. This microstructure provides high strength properties both at 20°C (yield strength up to 800 MPa) and at 650°C (yield strength up to 530 MPa). The values of elongation to failure remain at an acceptable level (5–8%). The grain structure formed in this work in austenitic steel EK-164 is more homogeneous than that after the earlier studied treatments.

Table 1. Mechanical properties of EK-164 steel.

State of the material	Temperature of tensile tests, °C	Yield strength, MPa	Tensile strength, MPa	Elongation to failure, %
ST [18]	20	201.4 ± 2	539.2 ± 9.6	47.4 ± 0.1
	650	95 ± 6.3	360.2 ± 8.8	31 ± 1.6
TMT-1	20	807.6 ± 9.2	983.9 ± 3	6.8 ± 0.9
	650	529.3	657.6	6.5
TMT-2	20	741.9 ± 18.7	831.3 ± 22.5	7.7 ± 0.2
	650	500.8 ± 11.8	576.6 ± 16.7	5.2 ± 0.1

Acknowledgements. The work was performed according to the Government Research Assignment for the Institute of Strength Physics and Materials Science of the Siberian Branch of the Russian Academy of Sciences (ISPMS SB RAS), project No. FWRW-2021-0008. The investigations have been carried out using the equipment of the Tomsk Regional Core Shared Research Facilities Centre of Tomsk State University and the Share Use Centre “Nanotech” of the Institute of Strength Physics and Materials Science SB RAS.

References

1. N.M. Mitrofanova, T.A. Churyumova. Problems of Atomic Science and Technology. 2 (98), 100 (2019). (in Russian)
2. A. Kozlov, K. Kozlov, I. Portnykh. J. Nucl. Mater. 549, 152915 (2021). [Crossref](#)
3. J. Zhao, Z. Jiang. Progr. Mater. Sci. 94, 174 (2018). [Crossref](#)
4. M. Eskandari, A. Najafizadeh, A. Kermanpur. Mater. Sci. Eng. A. 519, 46 (2009). [Crossref](#)
5. A. Järvenpää, M. Jaskari, A. Kisko, P. Karjalainen. Metals. 10, 281 (2020). [Crossref](#)
6. R. D. K. Misra, S. Nayak, P. K. C. Venkatasurya, V. Ramuni, M. C. Somani, L. P. Karjalainen. Metall. Mater. Trans. A. 41, 2162 (2010). [Crossref](#)
7. S. A. Akkuzin, I. Yu. Litovchenko, A. N. Tyumentsev, V. M. Chernov. Rus. Phys. Journal. 62, 698 (2019). [Crossref](#)
8. S. A. Akkuzin, I. Yu. Litovchenko. Vektor nauki Tolyattinskogo gosudarstvennogo universiteta. 2, 7 (2020). (in Russian) [Crossref](#)
9. S. J. Wang, T. Jozaghi, I. Karaman, R. Arroyave, Y. I. Chumlyakov. Mater. Sci. Eng. A. 694, 121 (2017). [Crossref](#)
10. H. Sun, Y. Sun, R. Zhang, M. Wang, R. Tang, Z. Zhou. Mater. Des. 64, 374 (2014). [Crossref](#)
11. M. S. Ghazani, B. Eghbali. Mater. Sci. Eng. A. 730, 380 (2018). [Crossref](#)
12. A. Dehghan-Manshadi, M. R. Barnett, P. D. Hodgson. Mater. Sci. Eng. A. 485, 664 (2008). [Crossref](#)
13. H. Mirzadeh, J. M. Cabrera, A. Najafizadeh, P. R. Cavillo. Mater. Sci. Eng. A. 538, 236 (2012). [Crossref](#)
14. I. Litovchenko, S. Akkuzin, N. Polekhina, K. Almaeva, E. Moskvichev. Metals. 11, 645 (2021). [Crossref](#)
15. Z. Yanushkevich, A. Lugovskaya, A. Belyakov, R. Kaibyshev. Mater. Sci. Eng. A. 667, 279 (2016). [Crossref](#)
16. Ch. Li, L. Huang, M. Zhao, X. Zhang, J. Li, P. Li. Mater. Sci. Eng. A. 797, 139925 (2020). [Crossref](#)
17. Z. Yanushkevich, S. V. Dobatkin, A. Belyakov, R. Kaibyshev. Acta Mater. 136, 39 (2017). [Crossref](#)
18. S. Akkuzin, I. Litovchenko, N. Polekhina, K. Almaeva, A. Kim, E. Moskvichev, V. Chernov. Metals. 12, 63 (2022). [Crossref](#)
19. S. A. Akkuzin, I. Yu. Litovchenko, A. N. Tyumentsev. AIP Conf. Proc. 2310, 020009 (2020). [Crossref](#)
20. V. Torganchuk, A. Belyakov, R. Kaibyshev. Mater. Sci. Eng. A. 708, 110 (2017). [Crossref](#)
21. E. Brünger, X. Wang, G. Gottstein. Scripta Mater. 38 (12), 1843 (1998). [Crossref](#)
22. A. Belyakov, H. Miura, T. Sakai. Mater. Sci. Eng. A. 255, 139 (1998). [Crossref](#)